Generalized parton distributions at CLAS

Silvia Pisano[a,*], for the CLAS Collaboration

[a] *Institut de Physique Nucléaire d'Orsay 15, Rue Clemenceau 91405 Orsay, France.*

Abstract

The understanding of the hadron structure in terms of QCD degrees of freedom is one of the main challenges of hadron physics. Indeed, despite the large amount of theoretical and experimental activity devoted to the subject in the last years, a full comprehension of mesons and baryons in terms of quark and gluon fields is still lacking. In order to operate a more detailed investigation of the hadron structure, new quantities have been introduced ten years ago, the Generalized Parton Distributions (GPDs), defined as bilocal, off-forward matrix elements of quark and gluon operators.
From an experimental point of view, GPDs are accessible through two main processes: Deeply Virtual Compton Scattering (DVCS) and Deeply Virtual Meson Electroproduction (DVMP). Depending on the polarization degrees of freedom acting in the process (like, for example, the simultaneous presence of a polarization in the beam and in the target, or the usage of a polarized beam with an unpolarized target), various combinations of GPDs can be accessed. In the case of DVCS, for example, the measurement of the Single Spin Asymmetry of processes like $e\vec{p} \rightarrow ep\gamma$ - realized by using a longitudinally polarized target - gives access to a combination of the GDPs H and $\tilde{H}$.
The *CEBAF Large Acceptance Spectrometer* (**CLAS**) installed in the Hall-B at JLab, is particularly suited for the extraction of these quantities. Its large acceptance implies a good capability in the reconstruction of exclusive final states, allowing the investigation of the aforementioned processes in a wide range of kinematics. In this presentation, an overview of the main GPD measurements performed by CLAS will be given. In particular, the first DVCS measurements realized both with unpolarized and polarized target, together with the measurements of some exclusive meson electroproduction processes, will be described.

Keywords: Hadronic physics, Generalized Parton Distributions, nucleon structure.

1. Introduction

A complete description of hadrons in terms of their elementary constituents, quarks and gluons, is one of the main challenges of the present hadronic physics. In spite of the large efforts devoted in the last decades to relate observed nucleon properties like mass, spin and electromagnetic form factors to its constituent behaviour, a full comprehension of such a translation is still missing. In order to gain a better understanding of the hadron properties (and in particular of the nucleon) a new tool has been introduced some decades ago, the so called *Generalized Parton Distributions* (**GPDs**) [1, 2], that, by combining the information coming from the electromagnetic form factors and from the standard parton distributions, allow a full, 3-dimensional description of the hadrons in terms of their partonic degrees of freedom. GPDs are defined as matrix elements of quark and gluon operators at a light-like separation (*i.e.* for a null light-cone time, $x^+ = x^0 + x^3 = 0$) [3, 4]. These functions depend on three variables: x, the quark longitudinal momentum fraction, ξ, the longitudinal fraction of the transfer four-momentum and t, the squared four-momentum transfer to the target. At the twist-two level, there are two spin-independent and two spin-dependent GPDs for each quark flavour, namely $H(x, \xi, t)$, $E(x, \xi, t)$ and $\tilde{H}(x, \xi, t)$, $\tilde{E}(x, \xi, t)$. First moments in x of the GPDs link them to the electromagnetic form factors, while $H(x, \xi = 0, t{=}0)$ and $\tilde{H}(x, \xi = 0, t{=}0)$ reduce to the quark longitudinal momentum and helicity distributions, respectively $q(x)$ and $\Delta q(x)$.
The best way to experimentally access these quantities is based on the so-called *"handbag"* mechanism and is represented by the *Deeply Virtual Compton Scattering* (**DVCS**) and the *Deeply Virtual Meson Produc-*

*Speaker
Email address: pisanos@jlab.org (for the CLAS Collaboration)

tion (**DVMP**). For DVCS with transverse photons and DVMP with longitudinal photons, indeed, a separation has been proved through the use of factorization theorems [1, 2, 6]: the underlying mechanism can be separated in a hard scattering part, well described through the tools of *Quantum ElectroDynamics* and/or *Quantum CromoDynamics*, and a non-perturbative part, that encodes the complex strong dynamics governing the existence of the hadron bound states and that is described with GPDs.

The actual extraction of GPDs through the DVCS process relies on the presence, in the $ep \to e'p'\gamma$ scattering, of a competitor mechanism producing the same DVCS final state, the so-called Bethe-Heitler process, where the final photon is emitted by the incoming or outgoing electron and not by the interacting quark. Due to its presence, indeed, the total amplitude for the process $ep \to e'p'\gamma$ turns out to be

$$A_{ep\to e'p'\gamma} = A^{BH} + A^{DVCS} \tag{1}$$

that at the cross-section level implies, besides the DVCS and the BH contributions, the presence of an interference term INT between them. In order to access to GPDs the three terms DVCS, BH and INT are isolated in the resulting cross-section and decomposed in spherical harmonics. The following asymmetry is then introduced:

$$A = \frac{d^4\vec{\sigma} - d^4\overleftarrow{\sigma}}{d^4\vec{\sigma} + d^4\overleftarrow{\sigma}}\,, \tag{2}$$

(the arrows corresponding to beam helicity +1 and −1) where only the interference term INT survives. INT, furthermore, turns out to be amplified by the presence of the Bethe-Heitler part, whose contribution is well calculated in the framework of the QED and can then be disentangled from the one from the DVCS, where GPDs appear. The asymmetry is related to the GPDs through $d^4\vec{\sigma} - d^4\overleftarrow{\sigma} \sim \sin\phi[F_1 H(\xi,\xi,t) + k_1(F_1+F_2)\tilde{H}(\xi,\xi,t) + k_2 F_2 E(\xi,\xi,t)]$, where F_1, F_2 are the Dirac and Pauli form factors of the nucleon, k_1, k_2 are kinematical quantities, and ϕ is the angle between the $\gamma^*\gamma$ plane and the electron scattering plane. At the leading twist, the asymmetry can then be written as

$$A = \frac{a\sin\phi}{1 + c\cos\phi + d\cos 2\phi}\,, \tag{3}$$

where the parameters a, c and d can be expressed in terms of harmonic coefficients for DVCS, BH and the interference between the two contributions. In particular, the coefficients for DVCS and INT can be expressed in terms of the so-called Compton Form Factors, $\mathcal{H}$, related to the GPDs through

$$\Re e\mathcal{H} = \mathcal{P}\int_{-1}^{1} dx \left[\frac{2x}{\xi^2 - x^2}\right] H(x,\xi,t)\,, \tag{4}$$

$$\frac{1}{\pi}\Im m\mathcal{H} = H(\xi,\xi,t) - H(-\xi,\xi,t)\,. \tag{5}$$

The asymmetry of Eq. 3 represents, then, the most suitable observable to extract the GPDs.

Another process adopted in the GDP extraction is the Deeply Virtual Meson Production. By measuring different channels a flavor-decomposition can be operated, allowing the access to the GPDs of every single quark flavour. One of the most suitable channel to access GPDs is $ep \to e'p\rho^0$. Predictions for the cross-section of this channel are indeed available both in terms of models based on the *hadronic* degrees of freedom, like those that make use of Regge theory (see Refs. [7–14]), and in terms of GPD models, that give description of the hadron dynamics in terms of *partonic* degrees of freedom (see Refs. [1–6, 15]). Among the hadronic descriptions, the one tested with the CLAS data is the so-called JML model ([7–10]), based on the Regge approach, according to which the reaction mechanism at the base of the meson electroproduction is the exchange of meson "trajectories" in the *t−channel*. On the other hand, as far as the GPD based models are concerned, their validity regime enters as soon as the Bjorken region is reached. An important topic is to understand what is the Q^2 value at which the validity of such a treatment starts. It will give information on the transition between the energy regime in which the hadron can be treated in terms of hadronic degrees of freedom and the one where a more elaborated, elementary "quantum field theory"-like approach starts to be needed.

2. Hall-B e1-dvcs experiment

The first Hall-B experiment devoted to the extraction of the DVCS beam-spin asymmetry (**BSA**) was the e1-dvcs experiment. It made use of a 5.77 GeV electron beam (with an average polarization $P = 0.794$), a 2.5 cm-long liquid-hydrogen target and the CEBAF Large Acceptance Spectrometer (**CLAS**) [16], operating at a luminosity of 2×10^{34} cm^{-2}s^{-1}. A new inner calorimeter (IC), located 55 cm downstream from the target, was added to the standard CLAS configuration, in order to detect the 1 to 5 GeV photons emitted between 4.5° and 15° with respect to the beam direction and obtain a fully exclusive final state reconstruction. All the three particles composing the $ep \to e'p'\gamma$ final

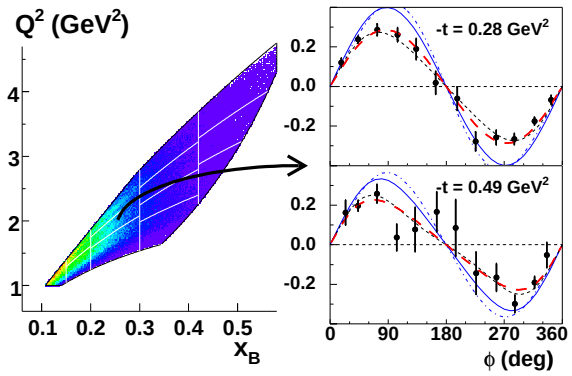

Figure 1: (Color online) Left: kinematic coverage and binning in the (x_B, Q^2) space (from Ref. [17]). Right: $A(\phi)$ for 2 of the 62 (x_B, Q^2, t) bins, corresponding to $\langle x_B \rangle$ = 0.249, $\langle Q^2 \rangle$ = 1.95 GeV^2, and two values of $\langle t \rangle$ (from Ref. [17]). The red long-dashed curves correspond to fits with Eq. (3) (with $d = 0$). The black dashed curves correspond to a Regge calculation [18]. The blue curves correspond to the GPD calculation described in the text, at twist-2 (solid) and twist-3 (dot-dashed) levels, with H contribution only.

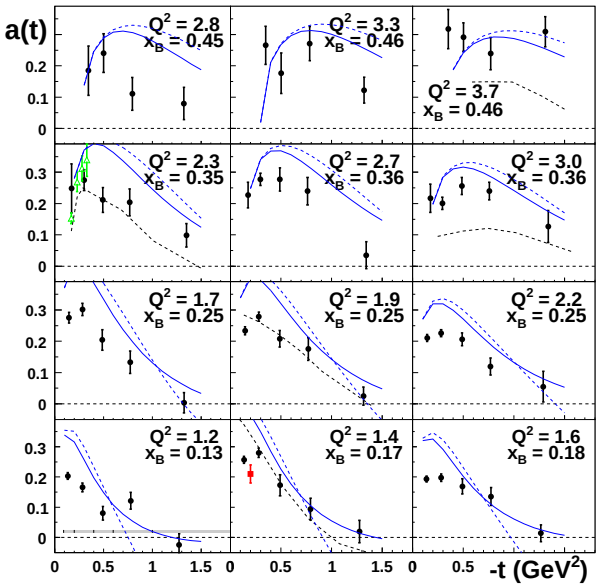

Figure 2: (Color online) $a = A(90°)$ as a function of $-t$. Each individual plot corresponds to a bin in (x_B, Q^2). Systematic uncertainties and bin limits are illustrated by the grey band in the lower left plot. Black circles are from Ref. [17]. Previous CLAS results are from Ref. [20] (red square) or extracted from cross section measurements [21] (green triangles), at similar - but not equal - values of $\langle x_B \rangle$ and $\langle Q^2 \rangle$. See Fig. 1 caption for curve legend.

state were detected, and the background was reduced through the application of exclusivity cuts. The data were divided into thirteen bins in the (x_B, Q^2) space as in Fig. 1, five bins in $-t$ (defined by the bin limits 0.09, 0.2, 0.4, 0.6, 1 and 1.8 GeV^2) and twelve 30° bins in ϕ. The parameter d in the denominator of Eq. 3 is expected to be smaller than 0.05 over our kinematic range, and indeed it was found compatible with zero within statistical accuracy when included in the fit. A couple of examples of the measured asymmetry are reported in Fig. 1, while in Fig. 2 $a = A(90°)$ as a function of $-t$ is shown. Together with the experimental data two fits are shown, one corresponding to the hadronic model proposed in Ref. [18], and the other corresponding to the GPD calculation in Ref. [14].

3. e1-6 experiment

The Hall-B e1-6 experiment measured the $ep \to e'p'\rho^0$ cross-section, by using a 5.754 GeV electron beam impinging on an unpolarized 5-cm-long liquid-hydrogen target (Ref. [22]). The integrated luminosity of the data was 28.5 fb^{-1}, with a kinematic domain corresponding approximately to Q^2 from 1.5 to 5.5 GeV^2, a $W > 1.8$ GeV (W being the $\gamma^* - p$ center-of-mass energy) and x_B ranging approximatively from 0.15 to 0.7. The transverse-longitudinal separation for $\sigma_{\gamma^* p \to p\rho^0}$ has been realized by analyzing the decay pion angular distribution in the ρ^0 center-of-mass frame and relying on the s-channel helicity conservation ($SCHC$, [19]).

The results for the cross-sections are in Fig. 3, that shows $\gamma_L^* p \to p\rho_L^0$ as a function of W for constant Q^2 bins, in units of μbarn, together with the world data. The dot-dashed curve superimposed to the data represents a fit obtained with the Regge JML calculation [7–10], while the dashed and the thin/thick solid curves represent fits obtained within GPD inspired models, in particular the VGG [11–14] and the GK [15] ones. In these last two models the (x, ξ) dependence of the H and E GPDs is described through a double distribution (cfr. Ref. [23]), but they differ in the t-dependence and in the way they sum up the two handbag contributions (*i.e.* the one due to the quark GPD and the one coming from the gluon part). In the GK case, indeed, the two diagrams are combined at the *amplitude* level, while in the VGG model the sum occurs at the *cross section* level (neglecting, in this way, the interference between the terms). By looking at the data in Fig. 3, two different behaviours can be appreciated for the cross-section: at low W σ_L decreases with W, while it starts to rise again at $W \approx 10$ *GeV*. The JML model reproduces fairly well these two general behaviours, but it drops as a function of Q^2 faster than the data and agrees only up to $Q^2 \approx 4.10$ GeV^2. The GPD-based models, on the other hand,

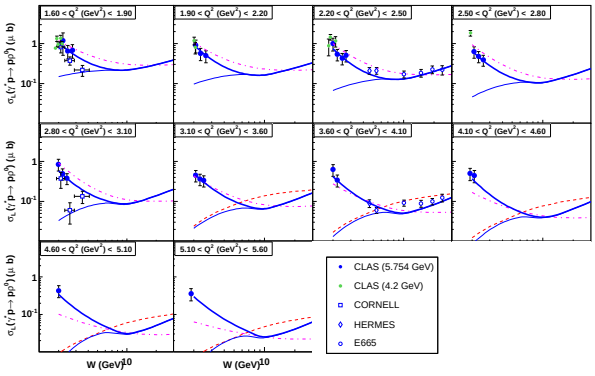

Figure 3: World data for the reduced cross sections of the reaction $\gamma_L^* p \to p\rho_L^0$ as a function of W for constant Q^2 bins, in units of μbarn. The dashed curve shows the result of the GK calculation and the thin solid curve shows the result of the VGG calculation. Both calculations are based on Double Distributions as proposed in Ref. [23] for the GPD parametrizations and incorporate higher twist effects through $k_\perp$ dependence. The thick solid curve is the VGG calculation with the addition of the D-term inspired contribution. The dot-dashed curve shows the results of the Regge JML calculation. The 4.2 GeV CLAS, CORNELL, HERMES and E665 data are respectively from refs. [24], [25], [26] and [27].

give a good description of the high and intermediate W region, down to $W \approx 5$ GeV. At high W the slow rise of the cross section is due to the gluon and sea contributions, while the valence quarks contribute only at small W. Since the VGG model miss the interference term, it differs the most from the GK model at intermediate W, where the inference is maximal, since it corresponds to the regime where the gluon contribution starts to play a role in the process, while the quark one is still significant. Both the GPD-based models fail to reproduce the low-W region. This can be due to a failure of the handbag description in this regime or to the presence of the meson amplitude (that represents a second, non-perturbative element) in the integrals defining the GPDs in the VGG and GK models.

4. Conclusions

GPDs are an essential tool in the comprehension of the nucleon structure and turn out to be particularly suitable to connect the observed degrees of freedom, namely hadrons, to the QCD-Lagrangian fields, *i.e.* quarks and gluons. The main processes to obtain an experimental access to these quantities are DVCS and DVMP. CLAS, the detector installed in the Hall-B at JLab, thanks to its large acceptance and the capability of a full, exclusive reconstruction of final states, is one of the most natural environment to measure this kind of processes. Results from the e1-dvcs experiment, based on the largest set of DVCS data currently available, show the expected sinusoidal dependence on ϕ for the beam-spin asymmetry, while the measure of the cross-section for the channel $ep \to e'p'\rho^0$ allows to test the phenomenological power of the present existing GPD models and to put constraints on them.

After the e1-dvcs experiment, another set of data has been taken in 2008 (e1-dvcs2), and new analysis are ongoing on these new data. Another experiment dedicated to DVCS has then been performed with a 6 GeV polarized electron beam and a polarized $^{14}NH_3$ target (eg1-dvcs experiment), to study single and double spin asymmetries in the DVCS process.

References

[1] X. Ji, Phys. Rev. Lett. **78** (1997) 610; Phys. Rev. D **55** (1997) 7114.
[2] J.C. Collins, L. Frankfurt and M. Strikman, Phys. Rev. D **56** (1997) 2982.
[3] M. Diehl, Phys. Rept. **388** (2003) 41.
[4] A.V. Belitsky and A.V. Radyushkin, Phys. Rept. **418** (2005) 1.
[5] A.V. Radyushkin, Phys. Lett. B **380** (1996) 417; Phys. Rev. D **56** (1997) 5524.
[6] D. Müller, D. Robaschik, B. Geyer, F.-M. Dittes, and J. Horejsi, Fortschr. Phys. **42** (1994) 101.
[7] J. M. Laget, Phys. Rev. D **70** (2004) 054023.
[8] J.-M. Laget, Phys. Lett. B **489** (2000) 313.
[9] F. Cano and J.-M. Laget, Phys. Rev. D **65** (2002) 074022.
[10] F. Cano and J. M. Laget, Phys. Lett. B **551** (2003) 317.
[11] M. Vanderhaeghen, P.A.M. Guichon, and M. Guidal, Phys. Rev. Lett. **80** (1998) 5064.
[12] M. Vanderhaeghen, P.A.M. Guichon, and M. Guidal, Phys. Rev. D **60** (1999) 094017.
[13] K. Goeke, M.V. Polyakov and M. Vanderhaeghen, Prog. Part. Nucl. Phys. **47** (2001) 401.
[14] M. Guidal, M.V. Polyakov, A.V. Radyushkin and M. Vanderhaeghen, Phys. Rev. **D72** (2005) 054013.
[15] K. Goeke, M. V. Polyakov and M. Vanderhaeghen, Prog. Part. Nucl. Phys. **47** (2001) 401.
[16] B. A. Mecking et al. Nucl. Instr. Meth. **A503** (2003) 513.
[17] F.X. Girod, Phys.Rev.Lett. **100** (2008) 162002.
[18] J. M. Laget, Phys. Rev. C **76** (2007) 052201.
[19] F. J. Gilman, J. Pumplin, A. Schwimmer and L. Stodolsky, Phys. Lett. B **31** (1970) 387.
[20] S. Stepanyan et al. Phys. Rev. Lett. **87** (2001) 182002.
[21] C. Muñoz Camacho et al., Phys. Rev. Lett. **97** (2006) 262002.
[22] S. Morrow et al., Eur. Phys. J. A **39** (2009) 5.
[23] A.V. Radyushkin, Phys. Rev. D **59** (1999) 014030; Phys. Lett. B **449** (1999) 81.
[24] C. Hadjidakis *et al.*, Phys. Lett. B **605** (2005) 256.
[25] D.G. Cassel *et al.*, Phys. Rev. D **24** (1981) 2787.
[26] A. Airapetian *et al.*, Eur. Phys. J. C **17** (2000) 389.
[27] M. R. Adams *et al.*, Z. Phys. C **74** (1997) 237.